ISSN: 1983 7402 ITA, 29 a 30 SET 2020

Microwave photonic Radar Warning Receiver (RWR) airborne antenna over fiber optic

Paulo Henrique Kiohara A. Bastos, Felipe Streitenberger Ivo, Olympio Lucchini Coutinho
Instituto Tecnológico de Aeronáutica (ITA), São José dos Campos – SP, Brazil.

***Abstract* — Electronic warfare was of great importance mainly in the second world war. Radar was one of the greatest inventions in the area at that time, reinventing the way war was viewed until then. Today, modern combat aircraft have sophisticated warfare systems, one of which is known as the Radar Warning Receiver (RWR), responsible for alert pilots to possible radar detection and guiding the direction in which it is being radiated. Technological innovations allowed the interaction of the Microwave and optoelectronics area, thus emerging an area known as Microwave Photonics (MWP). This article presents a photonic link to replace the copper cables used by RWR systems, thus applying photonic technology in order to improve performance and benefit from the intrinsic characteristics that optical fiber offers to the system, offering a totally passive remote system, where only one phase modulator is connected to the RWR antenna.**

***Key words* — Electronic warfare, Microwave Photonics, Radar Warning Receiver.**

I. INTRODUCTION

The concept of electronic warfare (EW) started with technological developments in the area of communication and detection, mainly during and after the second world war [1].

By definition, electronic warfare is divided in three areas: electronic attack, electronic protection and electronic support. Electronic attack basically involves deceiving and obstructing enemy communication radars. Electronic protection consists of limit electromagnetic signatures and protect military equipment from enemy electronic attacks. The electronic support has the function of detect radar emissions, locate and classify them as friend or enemy and supply those information to other EW systems, aircraft crew, as well as command and control and intelligence services [1, 2].

One system used as EW support in modern fighters is the Radar Warning Receiver (RWR). It is responsible to detect and characterize radar emissions and alerting the pilot when the aircraft is under detection [3,4]. This system has a set of antennas placed at strategic positions around the aircraft to get a wide coverage and to perform direction finding of the emission. EW systems usually operate at frequency bandwidth from 0.5 to 40 GHz, to detect radar pulses normally used in weaponry systems [4]. However, to achieve those functionalities, the antennas are often placed at positions where is difficult to launch coaxial cables and waveguides, as well as electric power supply wires.

Microwave Photonics (MWP) appear as a good solution to overcame those limitations, bringing the advantages of low electromagnetic propagations losses, low weight, small size and easily handle characteristics of fiber optic systems.

The Microwave photonics brings together two areas of knowledge: the microwave engineering and the optoelectronics. Initially, MWP was driven by telecommunications companies, reaching such levels of performance sufficient to draw the attention of military applications [5]. Microwave Photonics incorporates a series of photonic techniques into microwave engineering [6], improving the performance of communication systems and networks. MWP system can delivers relevant improvements in dynamic range, signal-to-noise ratio and bandwidth, among other advantages like electromagnetic immunity [7,8]. The use of this promising technology to transmit and to process RF signal over fiber have been gained attention on civil and military application, such as EW systems.

The main objective of this article is, through mathematic analysis and experiments, to demonstrate the concept of use MWP into airborne RWR system, proposing an all fiber optic solution for the receiving antennas system, in substitution to the coaxial cables transmission lines. The principle of operation of a phase-to-intensity RF over fiber link is presented in Section II. The proof of concept is experimentally demonstrated in Section III. An EW application experiment is introduced in Section IV. In Section V we conclude with the discussions and the conclusion.

II. PRINCIPLE OF OPERATION

A. *Phase-to-intensity modulation conversion microwave photonic link*

Fig. 1 shows the schematic diagram of the photonic link. The part called central station unit is where most photonic devices are located, leaving only the phase modulator (PM) isolated at the remote antenna probe area, that is, only the modulator and the RWR antenna will be positioned outside the controlled area.

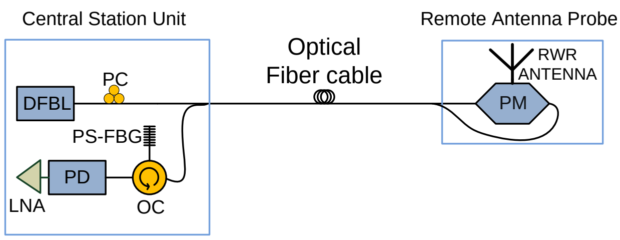

Fig. 1. Architecture of the proposed photonic link.

A Distributed Feedback Laser (DFBL) with a wavelength of 1551 nm is used, providing light as an optical carrier at the input of the phase modulator (PM), where the RF signal received by the antenna is then modulated. A

Paulo Henrique Kiohara A. Bastos, Kiohara@ita.br;Felipe Streitenberger Ivo, fivo@ita.br; Olympio Lucchini Coutinho, Olympio@ita.br.

polarization controller (PC) is used between the laser and the modulator, ensuring greater efficiency, since the phase modulator is sensitive to polarization.

The modulated signal then passes through an optical circulator (OC) where the signal is directed to the Phase Shift Fiber Bragg Grating (PS-FBG), where it undergoes the process of converting phase to intensity modulation (PM-IM). In addition, this PS-FBG can be used as a tunable microwave photonic filter (MPF) Fig. 2 (b) with ultra-fast tuning [8, 9].

The PM-IM conversion process is necessary since the photodetectors are only sensitive to variation in optical intensity. In the phase modulation, the beats between the sideband and carrier are canceled because they are out of phase [10]. When one of the first order sidebands enters the region known as notch of the PS-FBG, the amplitude and phase of this sideband is changed and the PM-IM conversion happens [11].

After the PM-IM conversion, the signal reflected by the PS-FBG passes through the OC again and is received by the photodetector (PD) and converted from an optical signal to an electrical signal. A low noise amplifier (LNA) is used to compensate the link losses.

The reflectivity spectrum of the Phase Shift Fiber Bragg Gratting (PS-FBG) is depicted in Fig. 2 (a), where it is possible to observe the notch of the grid and its lateral arms with their respective losses. The characterization of the used PS-FBG was carried out at the Laboratório de Guerra Eletrônica (LabGE) of Instituto Tecnológico de Aeronáutica and shows that it operates as a microwave photonic filter (MPF) with a bandwidth of 154MHz [8,12].

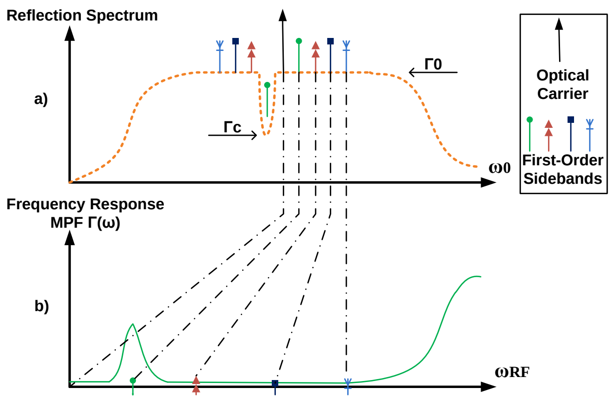

Fig. 2. Operating principle of the PS-FBG used for PM-IM conversion and used as a photonic filter.

In Fig.2 (a), Γ_c and Γ_0, are the reflectivity values given in dB, Γ_c being the notch value and Γ_0 filter arms and also represent optical losses, in this case by reflection, as part of the light is still transmitted.

B. *Link performance, gain, noise figure and frequency response.*

First, we must consider the carrier's optical signal, provided by the laser as expressed by [13]:

$$E(t) = E_0 e^{j(\omega_0 t)} \,, \tag{1}$$

where E_0 is the optical carrier amplitude, ω_0 is its angular frequency.

The modulating RF signal provided by the antenna is injected into the modulator, expressed as [13]:

$$v_{rf}(t) = V_{rf} \cos(\omega_{rf} t) \,, \tag{2}$$

where ω_{rf} and V_{rf} are respectively the angular frequency and the amplitude of the RF modulating signal.

After the phase modulation is performed, assuming that the optical carrier with an angular frequency ω_0 enters the phase modulator, where the RF modulating signal expressed by (2) modulates the light, the electric field at the output of the modulator is given by [13]:

$$E_{OUT}(t) = K_0 E_0 e^{j(\omega_0 t+\emptyset_b)} \sum_{n=-\infty}^{n=\infty} (j)^n J_n(m)\, e^{-jn(\omega_{rf} t)}, \tag{3}$$

where K_0 are the optical losses up to the modulator output, $\emptyset_b$ is the phase shift of modulated signal, m is the modulation index and J_n it is the Bessel function of the first kind of order n. In (4), m is defined by [13]:

$$m = \frac{\pi V m}{V\pi} \,. \tag{4}$$

The PM output signal is injected into the PS-FBG where the spectrum symmetry breaks and the PM-IM conversion process occurs. The resulting IM modulated optical signal is then injected into the photodetector. Then the electric field at the input of the photodetector is given by:

$$E_{pd}(t) = K_t E_0 e^{j(\omega_0 t+\emptyset_b)} \sum_{n=-\infty}^{n=\infty} (j)^n J_n(m)\, \Gamma(\omega) e^{-jn(\omega_{rf} t)}, \tag{5}$$

where K_t represents all optical losses of the link and $\Gamma(\omega)$ is the frequency response in amplitude of the PS-FBG photonic filter (MPF) described in Fig.2 (b).

We can then determine the optical intensity in the photodetector given by the following expression [8]:

$$I_d \propto E_{pd} E_{pd}^{*} . \tag{6}$$

The photodetector current I_d is proportional to the optic intensity. So, the microwave output signal can be recovered at this point. Considering a small signal condition, where m<<1, the PM-IM photonic link power intrinsic gain G is expressed by [8,14]:

$$G = {P_{od}}^2 \left(\frac{\pi\eta}{V\pi}\right)^2 {F_c}^2 \left(\frac{Z_d}{Z_d+Z_l}\right)^2 Z_m Z_l, \tag{7}$$

where P_{od} is the optical power in the photodetector already considering all the optical losses of the link, η is the responsivity of the photodetector, $V\pi$ is the half-wave voltage of the modulator, Z_d the photodetector impedance, Z_l its load impedance and Z_m is the impedance of the modulator.

We define F_c as the phase to intensity modulation conversion factor (PM-IM), given by:

$$F_c = \left(1 - \frac{\sqrt{\Gamma_0 \Gamma_c}}{\Gamma_0}\right). \tag{8}$$

Substituting (8) into (7), and considering G_{LNA} as the gain of the LNA placed after the photodetector, we can then calculate the total gain G_t of the system as:

$$G_t = G_{LNA} {P_{od}}^2 \left(\frac{\pi\eta}{V\pi}\right)^2 \left(1 - \frac{\sqrt{\Gamma_0 \Gamma_c}}{\Gamma_0}\right)^2 \left(\frac{Z_d}{Z_d+Z_l}\right)^2 Z_m Z_l. \tag{9}$$

Another important parameter to consider in order to measure the performance of a photonic link is its Noise Figure [14-16]:

$$NF_L = 10\log\left[P_{re} + \frac{2|e|P_{od}\eta}{K_bTG} + \frac{\eta^2 P_{od}^2 rin}{K_bTG} + \frac{1}{G}\right], \qquad (10)$$

where K_b is the Boltzmann constant, T is the temperature in Kelvin, e is the electron charge, P_{od} incident optical power in the photodetector, η is responsivity of the photodetector, rin its laser relative intensity noise and G is the gain of the link without amplification, expressed in (7).

The total NF of the link with post amplification is given by:

$$NF = NF_L + 10log\left[\left(\frac{F_a - 1}{G}\right)\right], \qquad (11)$$

where F_a is the amplifier noise factor and G is the photonic link gain in decimal.

III. EXPERIMENT

The experiment was carried out at the *Laboratório de Guerra Eletrônica* (Electronic Warfare Laboratory - LAB-GE) of the *Instituto Tecnológico de Aeronáutica* (Technologic Institute of aeronautics – ITA). All components used in the experiments were experimentally characterized at the laboratory. Fig. 3 shows all the devices used in the experiment.

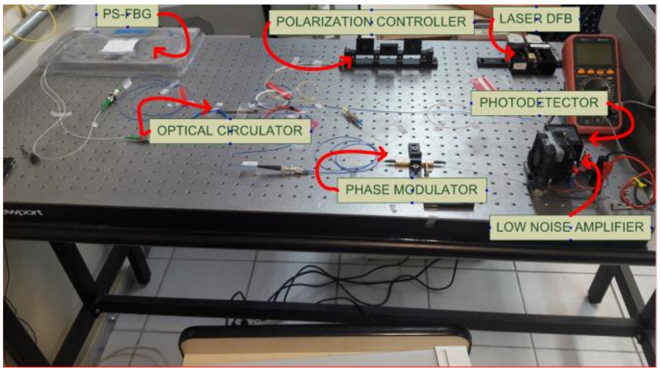

Fig. 3. Experimental Optical Link.

The DFB laser delivers a maximum optical power of 100mW and was characterized using an optical spectrum analyzer . The used phase modulator is from Covega Inc.

The V_π measurement of the PM was obtained adjusting the RF signal amplitude, V_m, to obtain $J_0 = J_1$ approximately 1.42. This value can be acquired directly through the graph of the Bessel functions [17]. The RF power at the modulator output was then measured and thus obtaining a modulation voltage V_m of 3V using Eq. 1 it is possible to obtain the voltage $V\pi$ of the phase modulator, the measured Vπ is 6.67V. The equipment used to carry out the measurement were an Agilent Technologies E8257D RF generator (bandwidth 250kHz to 20GHz) and a E4407B ESA-E Spectrum Analyzer (bandwidth 9kHz to 26.5GHz).

The used photodetector is from New Focus Inc (bandwidth 25GHz) and its maximum incident power is 4.3mW, with a measured responsivity of 0.56A/W.

The schematic diagram of the link and the decomposition of the corresponding optical losses are shown in Fig. 4.

Losses were measured point to point, obtaining a total value of 6.87dB, 0.3dB losses come from each PC to PC and APC to APC connectors.

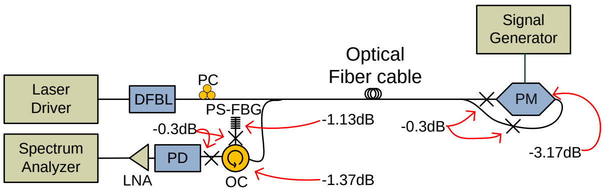

Fig. 4. Schematic diagram and losses.

The components shown in Fig. 5 are basically the same as those presented in section II, Fig. 1, adding just three essential equipments for measurement: the Thorlabs model ITC 510 laser driver, the Agilent PSG Analog Signal Generator 250kHz- 20GHz and the Agilent MXA Signal Analyzer 20Hz-26.5GHz.

Fig. 5 shows the theoretical results disregarding the performances of the microwave photonics link (NF and G) depending on the received optical power at the input of the photodetector.

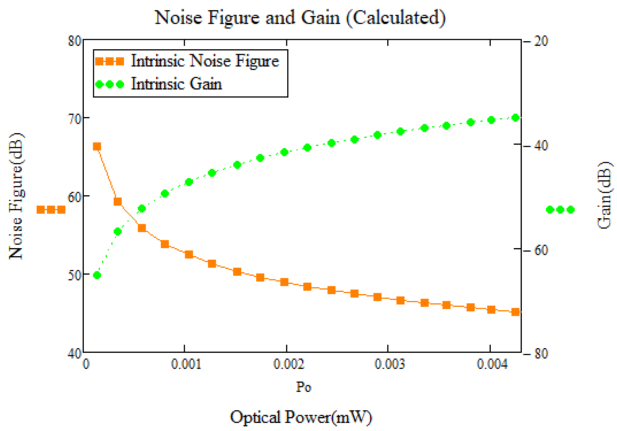

Fig. 5. Calculated Gain and Noise Figure.

However, the experiment was performed in the 500MHz-3GHz band, the performances of the system were very close to those calculated in session II. The measured Gain showed a maximum variation of 0.2dB in relation to the calculated one.

The Noise Figure presented variations of up to 1.5 dB, mainly due to difficulties with the sensitivity of the equipment for this type of measurement.

The results of the characterization can be seen in Fig. 6, considering the values disregarding the LNA. Fig. 7 demonstrates the enhanced gain obtained for the total link G_t, using a LNA with a gain of 42dB, with respect to the intrinsic gain of the link.

The maximum value is obtained for 4.3mW of incident optical power on the photodetector and is around -35dB of gain, reaching 7dB with the use of the LNA.

The system also responded well in frequency. Fig. 8 shows the gain in frequency (S21) and reflectivity (S11), considering the amplification of 42 dB of the LNA too; the measurements were performed between 500 MHz and 3GHz.

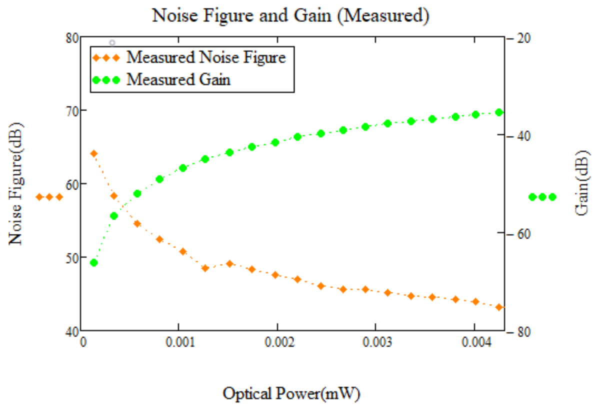

Fig. 6. Measured Noise Figure and Gain.

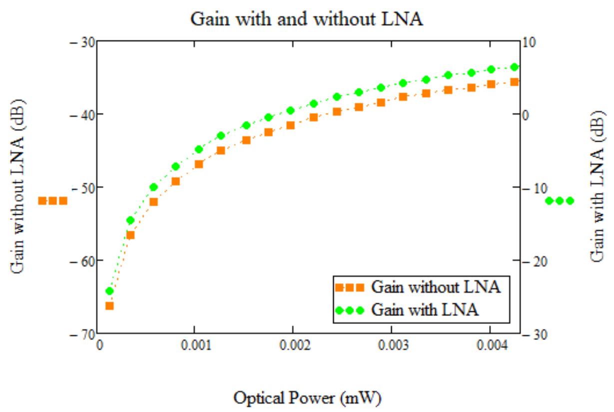

Fig. 7. Gain with and without LNA.

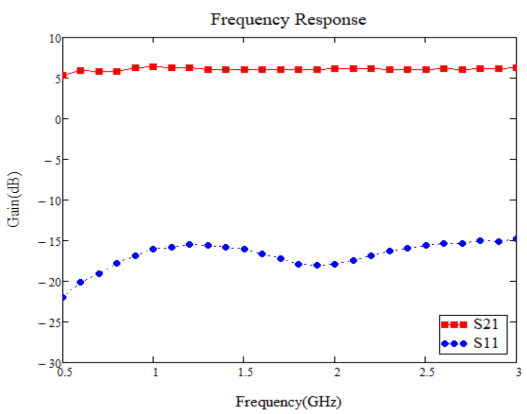

Fig. 8. Link Frequency Response.

IV. APPLICATION

Fig. 9 shows an example of the distribution of RWR antennas on the aircraft. Once the signal is detected by the RWR antenna, it is transmitted to the Central Station Unit (CSU) to be processed, identifying and giving the exact direction of emission [3].

The antennas of the RWR system are positioned in strategic places on the aircraft, playing an essential part of the system [3]. Usually coaxial cables are used to transport the radar signals from the RWR Antennas to the CSU. However, coaxial cables are susceptible to electromagnetic interference, which is also one of the major problems faced by RWR systems [3].

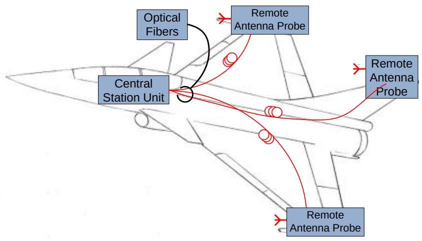

Fig. 9. Simplified RWR system.

So, the opportunity to benefit from one of the main intrinsic characteristics of optical fiber systems which is their electromagnetic immunity, is of great importance here.

Some tests were carried out in an appropriate environment at the LabGE-ITA, to verify the possibility of using this system in a real application of an airborne RWR antenna.

The proposed experiment is the replacement of coaxial cables by optical fibers and the positioning of the phase modulator directly at the output of the RWR antenna. Thus, this creates a totally photonic transmission medium, with the additional interest to be a fully passive system, not requiring feeding power in this case. Fig. 10 shows the experiment configuration of the transmitting and receiving antennas.

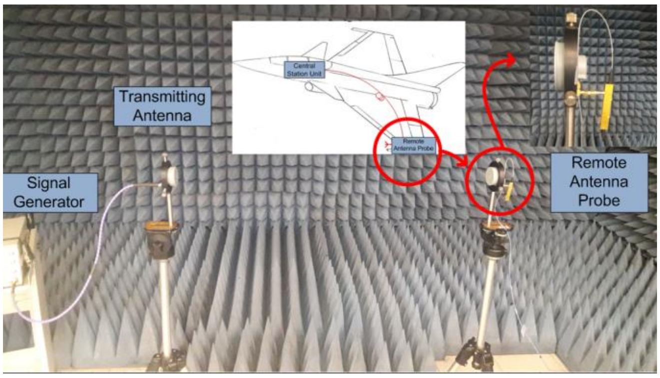

Fig. 10. Photonic remote RWR antenna experiment.

The antenna and the phase modulator set correspond to one of the positions of the aircraft's RWR remote antenna probe. Where the antenna connection with the CSU is totally photonic, the rest of the link remains the same as in Fig. 4.

The antennas are positioned one meter from each other in a suitable place. A pulsed signal with a width of 1μs and a period rate of 1ms are transmitted by the signal generator. Fig. 11 illustrates the pulse with its respective period.

For a pulsed signal with input power of 16 dBm at 3GHz, it was possible to detect an output signal close to -38 dBm as shown in Fig. 12 by using a 42 dB gain LNA post amplifier. It is a weak signal compared to that presented in session 3. It is important to emphasize that both links have the same parameters and this drop is due to irradiation loss.

Due to the loss, the signal-to-noise ratio is around 10 dB, that is, the link is operating near its detection limit it is possible to observe this in the frequency spectrum in Fig. 13.

It is important to emphasize that the Gain of the microwave photonics link can be optimized by increasing the optical power, but the limitation is mainly in the allowed maximum optical input power of the photodetector.

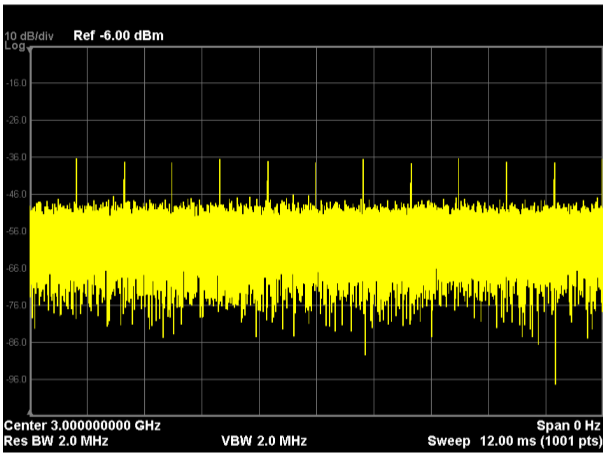

Fig. 11. Zero span signal with 1ms of period.

Fig. 11 illustrates the pulse with its respective width.

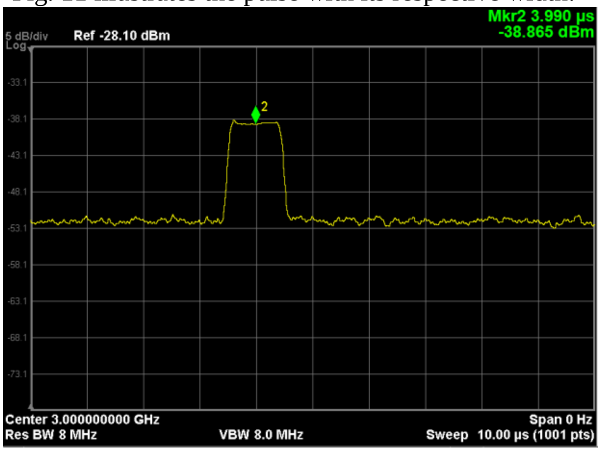

Fig. 12. Zero Span signal with 1µs width.

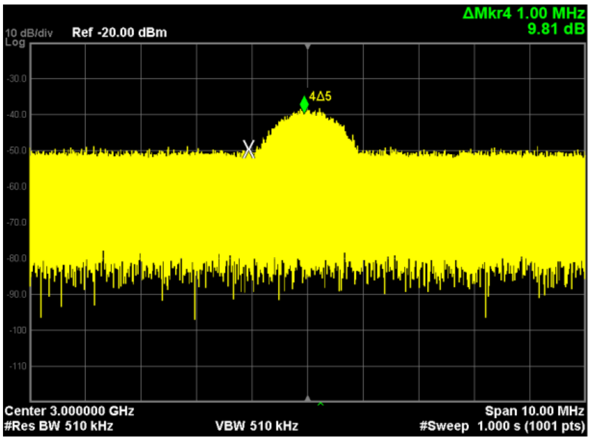

Fig. 13. Maximum output power on the spectrum analyzer.

V. Discussions and Conclusion

The results presented in this paper demonstrate the efficiency of the microwave photonics link to transmit with good performances the RWR signal, offering satisfactory results in relation to signal noise and system gain, reaching values close to 10dB for the gain of the link with post-amplification, and with less than 50% of the photodetector's optical capacity.

The result of the practical test in section 4, in spite of the losses due to irradiation, the link presented a expected result, confirming that it is totally possible to use a photonic link to replace the coaxial cables used today in RWR systems, providing the intrinsic advantages when using this technology.

The low noise amplifier was used in a post-amplification configuration in order to avoid the need of electric power supply at the remote antenna probe. So, it only compensates the link gain, but not the noise figure. To solve this problem and to reduce the NF, we consider now to have a remote LNA at the RWR antenna, and to use the Power Over Fiber technology to feed it [18]. This ongoing research is carried out in cooperation between the microwave photonics research group at the Technologic Institute of aeronautics (ITA, Brasil) and the photonics research group at the École Nationale d'Ingénieurs de Brest (ENIB, France).

Acknowledgment

This research is supported by Capes, the Brazilian Air Force and the École Nationale d'ingénieurs de Brest (ENIB), in the framework of a joint research project in Microwave Photonics between ENIB and ITA(Ref. MWP-ITA-ENIB 2020 project).

References

[1] G. Ricardo, "Guerra cibernética / Guerra electronica- conceitos, desafios e espaços de interação", Revista Política Hoje - Volume 26, n. 1 2017.

[2] Congressional Research Service,"U.S. Airborne Electronic Attack Programs: Background and Issues for Congress", May 14, 2019.

[3] W. Richard, "ELINT The Interception and Analysis of Radar Signals", Artech House, 2006.

[4] N. Filippo, "Introduction to Electronic Defense Systems", Second Edition Artech House, Boston, London, 2006.

[5] H. Charles, A. Edward, "Microwave Photonics: Past, Present and Future", Billerica, MA, USA, IEE, 2008.

[6] M. Carla, "Avanços Recentes em Optoeletrônica Aplicada a Radares e Guerra Eletrônica", Departamento de Microondas e Optoeletrônica – Instituto Tecnológico de Aeronáutica.

[7] C. José, "Microwave photonics combines two worlds" Nature Photonics, 2007.

[8] I. Felipe, "Filtro de RF Sintonizável Baseado em Processamento Fotônico com Varredura Ultrarrápida", Departamento de Eletrônica, – Instituto Tecnológico de Aeronáutica, 2018.

[9] C. José, M. José, G. Ivana, S. Juan, L. Juan, S. Salvador, " Microwave Photonics Signal Processing" IEEE Journal of Lightwave Technology, 2013.

[10] A.Yariv, P. Yeh "Photonics optical electronics in modern communications", New York, Oxford University, 2007.

[11] W. Li, M.Li, J. Yao, "A Narrow-Passband and Frequency-Tunable Microwave Photonic Filter Based on Phase-Modulation to Intensity Modulation Conversion Using a Phase-Shifted Fiber Bragg Gratting" IEEE Transactions on Microwave Theory and Techniques, 2012.

[12] I. Felipe, R.F. Baroni, C.Olympio. "Filtro de RF Fotônico Sintonizável por Variação de Temperatura em Laser DFB", Simpósio de Aplicações Operacionais de Defesa 19, São José dos Campos, 2017.

[13] A. Yariv. P. YEH, "Optical Waves in Crystals", New York, John Wiley & Sons 1984.

[14] C. Olympio, "Aplicação de Moduladores Eletroopticos em Enlaces Analógicos a Fibra Óptica", Departamento de Eletrônica, – Instituto Tecnológico de Aeronáutica, 2005.

[15] C. Olympio; O. José, "Enlace analógico a fibra óptica para transmissão de sinais de RF", SIMPÓSIO DE GUERRA ELETRÔNICA, 6, São José dos Campos, 2004.

[16] E. Ackerman, C. COX. "State of Art in Analog Fiber-Optic Link Technology", Signals, Systens, and Electronics, 1998.

[17] S.Jerome, O. Keith, "An atlans of functions" Hemisphere publishing corporation 1987.

[18] Cherif Diouf et al. "Design, Characterization, and Test of a Versatile Single-Mode Power-Over-Fiber and Communication System for Seafloor Observatories", IEEE Journal of Oceanic Engineering (Nov. 2018), url: https : / / hal.archives-ouvertes.fr/hal -01990925.